

A Quick & Dirty Guide to Astrophysical Molecular Rotation Spectroscopy

Yancy L. Shirley

NRAO, P.O. Box 1, Socorro, NM, 87801 USA

yshirley@nrao.edu

1. Introduction

1.1. Motivation

This is a quick and dirty guide to molecular spectroscopy. It is meant to be used as a tool for learning and remembering which rotational lines exist and can be observed. Nothing can supplant the excellent discussion in Townes & Schawlow's *Molecular Spectroscopy* (1975) and Gordy & Cook's *Microwave Molecular Spectra* (1984) (hereafter TS75 and GC84). If you wish to understand the details, you should look at these two books first. With this guide I hope to fill in some the pedagogical gaps that I encountered while learning this subject. Nothing helps me learn faster and with better retention than examples, examples, examples! Therefore, for every case discussed, I have included at least one (if not more) astrophysically observed examples with energy level diagrams and a discussion of why the rotational spectrum looks the way it does.

I have broken down the guide into 3 main sections: linear molecules, symmetric top molecules, and asymmetric top molecules in electronic states with no projected electronic orbital or spin angular momentum. Eventually, I shall write a section on molecules with electronic angular momentum (specifically $^2\Sigma$, $^3\Sigma$, and $^2\Pi$ states). Each section has a subsection on hyperfine structure for that particular type of molecule.

All of the spectroscopic data is from the JPL line catalog (<http://spec.jpl.nasa.gov/>), Lovas line catalog (<http://physics.nist.gov/cgi-bin/micro/table5/start.pl>) and Cologne Spectroscopy Database (<http://www.ph1.uni-koeln.de/vorhersagen/>). These webpages are extremely useful. I have used them on many occasions at the telescope (for instance, to check to see what lines may lie in the opposite sideband). I hope that this proves to be a useful guide.

1.2. Permanent Electric Dipole Moments

The vast majority of molecular rotation spectra observed are due to a electric dipole transition in molecules that have a permanent electric dipole moment. A molecule has a permanent electric dipole moment, μ , if there is a charge imbalance in the molecule. Molecules which are highly

symmetric, such as H_2 , N_2 , O_2 , and CH_4 do not have permanent dipole moments. Figure 1 shows examples of molecules with and without permanent electric dipole moments.

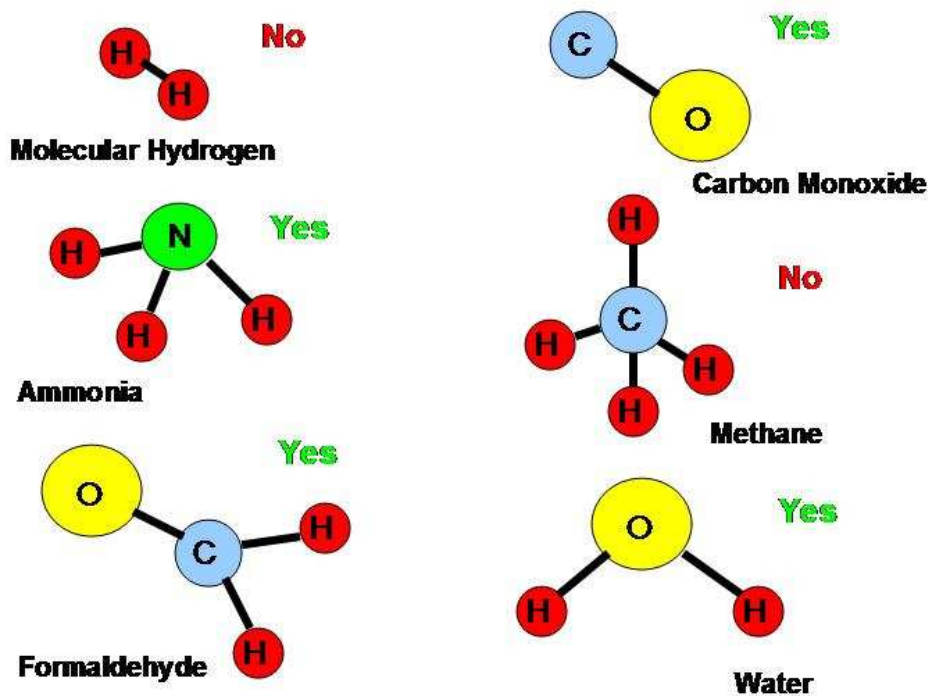


Fig. 1.— Molecules with charge imbalances have permanent electric dipole moments. A green YES denotes a permanent electric dipole moment and a red NO denotes no permanent electric dipole moment. The top row shows linear molecules H_2 and CO . The second row shows symmetric top molecules NH_3 and CH_4 . The third row shows asymmetric top molecules H_2CO and H_2O .

1.3. Basic Molecular Shapes

An orthogonal coordinate system can always be found such that the moment of inertia tensor, $\overset{\leftrightarrow}{I}$, is diagonal (see Marion & Thornton 1988, Classical Dynamics, §10.4). Molecular shapes are always classified in this coordinate system by the non-zero diagonal components of $\overset{\leftrightarrow}{I}$: I_x , I_y , and I_z . There are four fundamental shapes: linear ($I_x = I_y, I_z = 0$), symmetric top ($I_x = I_y < I_z$ or $I_x < I_y = I_z$), spherical top ($I_x = I_y = I_z$), and asymmetric top ($I_x \neq I_y \neq I_z \neq 0$).

1.4. Electric Dipole Transitions

The parity of the wavefunction, or the symmetry of the wavefunction after inversion of the coordinate system $(x, y, z) \rightarrow (-x, -y, -z)$, is extremely important for determining the multipole of radiation in a transition. Nearly all astrophysically important molecular transitions are electric dipole. From Figure 2, we see that electric dipole transitions require the two rotational levels to be antisymmetric with respect to each other. The symmetry properties of the rotational levels will determine which transitions exist and therefore determine the selection rules.

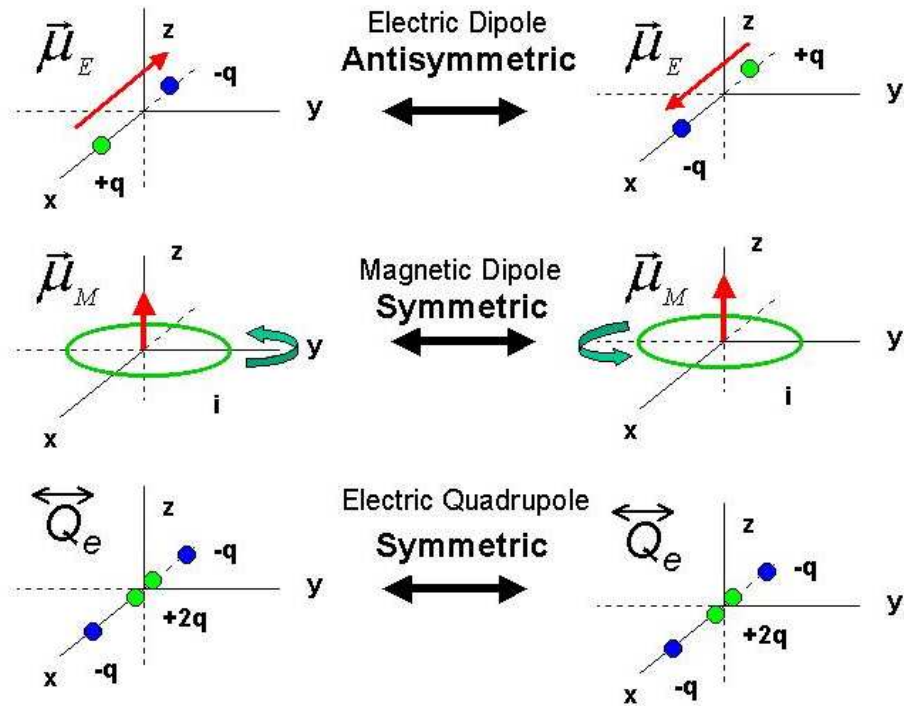


Fig. 2.— The Parity of electric dipole, magnetic dipole, and electric quadrupole transitions are shown. The axes on the right represent an inversion of the coordinate system.

2. Linear Molecules – $^1\Sigma$ Electronic State

2.1. Rotational Spectrum

A linear molecule has all of its nuclei along a single symmetry axis of the molecule. We can understand the basic rotational spectrum by modeling the molecule as a rigid rotor (i.e. no vibration or stretching and the distance of each nucleus remains fixed with respect to the center-of-mass). The Hamiltonian is defined by

$$H = T + V, \quad (1)$$

where T is the kinetic energy and V is the potential energy. We will set the potential energy equal to zero ($V = 0$). Classically, we find the kinetic energy of a rotating system to be

$$T = \frac{\vec{J}^2}{2I}, \quad (2)$$

where \vec{J} is the angular momentum and I is the moment of Inertia of the molecule. We simply replace the angular momentum, \vec{J}^2 , in equation (2) with the quantum mechanical operator, \hat{J}^2 , to form the rotational Hamiltonian

$$\hat{H}_{rot} = \frac{\hat{J}^2}{2I}, \quad (3)$$

where we have ignored electronic and vibrational motions (the Born-Oppenheimer approximation).

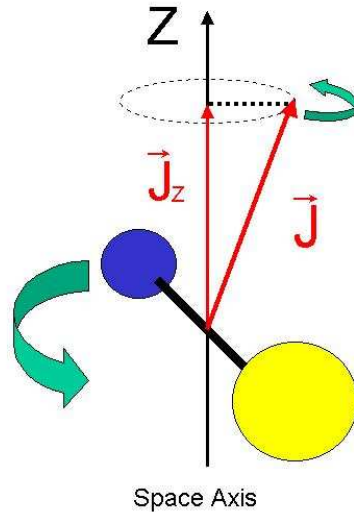


Fig. 3.— The vector model for a rotating linear molecule.

Quantum mechanics tells us that when we operate on a wavefunction with the Hamiltonian and angular momentum operators, we find

$$\hat{H}_{rot}\Psi = E\Psi \quad (4)$$

$$\hat{J}^2\Psi = \frac{h^2}{4\pi^2}J(J+1)\Psi \quad (5)$$

$$\hat{J}_Z\Psi = hM_J\Psi, \quad (6)$$

with J equal to the rotational quantum number and \vec{J}_Z denotes the projection of the total angular momentum on a fixed axis in space, which we will denote Z (see Figure 3). The rotational wavefunction is described by quantum numbers J and M_J . Using Dirac notation we can write $\Psi = |JM_J\rangle$.

When we discuss molecules with electronic angular momentum, the rotational angular momentum of the nuclear framework is denoted \vec{O} instead of \vec{J} . \vec{J} is reserved for the total rotational **and** electronic orbital angular momentum. Only when the projection of the electronic orbital angular momentum on the bond axis and total electronic spin angular momentum are zero ($\Lambda = 0$ and $S = 0$) is $\vec{J} = \vec{O}$ (i.e. a $^1\Sigma$ state). However, J is traditionally used for linear molecules in $^1\Sigma$ states.

The rotational energy levels are found by substituting the eigenvalue of \hat{J}^2 (Equation (5)) into the rotational Hamiltonian operator (Equation (3)) to give

$$E = \frac{h^2}{8\pi^2I}J(J+1) = hBJ(J+1), \quad (7)$$

where $B = \frac{h}{8\pi^2I}$ is the molecular rotation constant (N.B. in Dirac notation $E = \langle JM_J | \hat{H}_{rot} | JM_J \rangle$). The selection rule for electric dipole transitions of linear molecules in the $^1\Sigma$ state is $\Delta J = \pm 1$. The frequency of a transition from $J = J+1 \rightarrow J$ is

$$\nu_{J+1 \rightarrow J} = \frac{E_{J+1} - E_J}{h} = 2B(J+1). \quad (8)$$

In reality, the energy levels of a linear molecule are modified by centrifugal stretching and vibrations of the nuclei about their equilibrium positions. These modifications are generally minor but very important for accurate calculations. The first order correction for centrifugal distortion is $-DJ^2(J+1)^2$, with D on the order of a few hundred kHz (see Atkins & Friedman 1997, *Molecular Quantum Mechanics*, §10.4). The rotational constant, B , is on the order of a few tens of GHz (see Table 1). The corrections become more important at higher J levels as the centrifugal distortion is proportional to J^4 .

In the rigid rotor approximation, we can see two important aspects of the rotational spectrum of linear molecules. The energy levels are spaced quadratically ($E = 0, 2B, 6B, 12B, \dots$). The frequency of transitions with $\Delta J = -1$ are spaced linearly ($\nu_{J+1 \rightarrow J} = 2B, 4B, 6B, \dots$). This latter property is extremely useful for gauging the frequency for higher J transitions (e.g. the $J = 1 \rightarrow 0$ CO transition is at 115 GHz; therefore, $J = 2 \rightarrow 1$ is at 230 GHz and $J = 3 \rightarrow 2$ is 345 GHz, etc.). Table 1 lists the rotational constant, B , and electric dipole moment, μ , for many astrophysically observed linear molecules. Figure 4 shows the energy level diagrams for some example linear molecules.

Linear Molecule $^1\Sigma$ Example Rotational Spectra

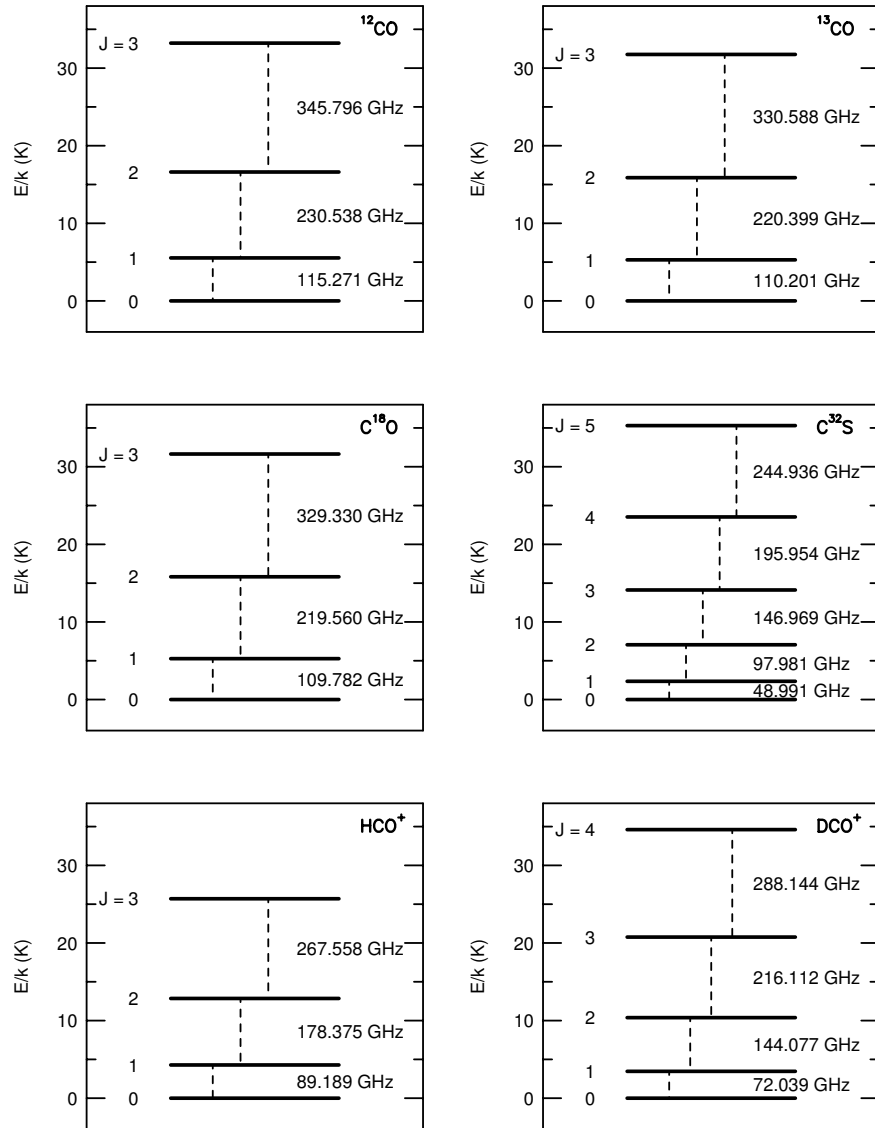


Fig. 4.— The energy level diagram of CO , ^{13}CO , C^{18}O , CS , HCO^+ , and DCO^+ for all energy levels less than 40 K above the ground state. The vertical axis is the energy above ground, E/k , in K. All energy level diagrams are plotted on the same vertical scale. Notice that heavier molecules, such as CS , have more closely spaced energy levels.

2.2. Hyperfine Structure - Linear $^1\Sigma$ State

2.2.1. Single Coupling Nucleus

Hyperfine structure is due to two separate interactions: electric quadrupole and magnetic hyperfine coupling. Typically, electric quadrupole coupling is much stronger for molecules in $^1\Sigma$ states. For nuclei with nuclear spins, I , equal to 0 or $1/2$, the nuclear charge distribution is spherically symmetric and there is no electric quadrupole moment. Nuclei with nuclear spin greater than $1/2$ have electric quadrupole moments. The nuclear electric quadrupole moment couples with the gradient of the electric field at the nucleus. Nuclei with a nuclear spin greater than 0 can have a dipole magnetic moment. Magnetic hyperfine coupling is the coupling between the nuclear magnetic moment and the magnetic field generated by molecular rotation. Table 2 and Figure 4 list nuclear spins for nuclei commonly found interstellar molecules. Hyperfine structure is commonly observed in molecules that contain H ($I = 1/2$), D ($I = 1$), ^{14}N ($I = 1$), and ^{17}O ($I = 5/2$) nuclei (see Figure 4).

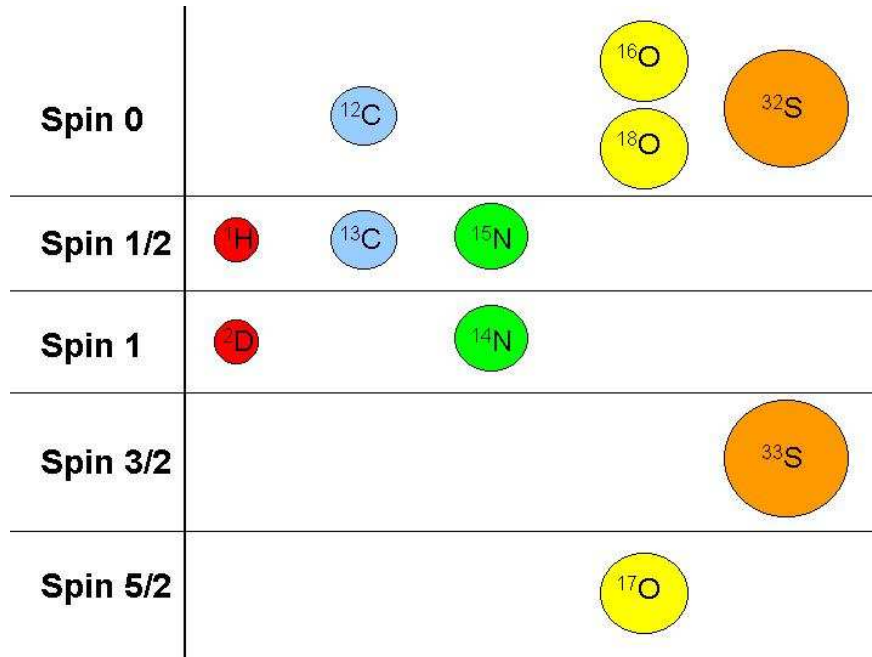


Fig. 5.— The spin of nuclei in common astrophysically observed molecules.

The hyperfine quantum number, F , is defined such that $\vec{F} = \vec{I} + \vec{J}$ is the total molecular angular momentum, where \vec{I} and \vec{J} are the nuclear spin and rotational angular momentum of the molecule respectively (\vec{I} and \vec{J} precess around \vec{F} ; see Figure 6). Then,

$$\vec{F}^2 = (\vec{I} + \vec{J})^2 = \vec{I}^2 + \vec{J}^2 + 2\vec{I} \cdot \vec{J}, \quad (9)$$

$$F = J + I, J + I - 1, \dots, |J - I|. \quad (10)$$

Equation (10) is sometimes called a Clebsch-Gordan series.

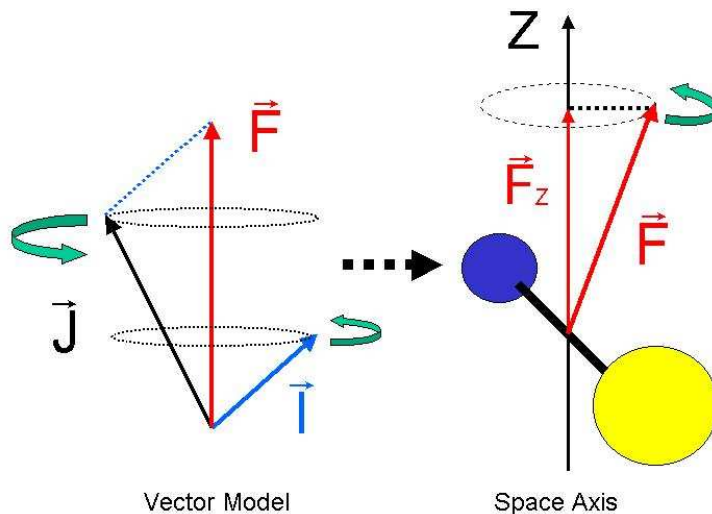


Fig. 6.— The vector model for the hyperfine structure of a linear molecule in a $^1\Sigma$ state.

Selection rules stipulate that $\Delta F = 0, \pm 1$ and $\Delta J = \pm 1$. Equation (10) determines which hyperfine levels exist and the selection rule determines which transitions exist. I shall discuss the hyperfine energy level structure for HCN ($I(^{14}\text{N}) = 1$) and C^{17}O ($I(^{17}\text{O}) = 5/2$). Almost all hyperfine structure in linear molecules in a $^1\Sigma$ state can be understood from these two examples!

The ^{14}N nucleus in HCN is responsible for strong hyperfine coupling (N.B. in Table 2, ^{14}N has the strongest electric quadrupole moment by a factor of 4). The spin of ^{14}N is $I = 1$. Equation (10) shows that the $J = 0$ level remains unsplit ($F = 1$), the $J = 1$ level splits into a triplet ($F = 2, 1, 0$), and the $J = 2$ level also splits into a triplet ($F = 3, 2, 1$). The selection rule allows 3 transitions from $J = 1 \rightarrow 0$ and six hyperfine transitions from $J = 2 \rightarrow 1$. Since $I = 1$ and the Clebsch-Gordan series (equation (10)) terminates with $F = |J - I|$, all of the levels with $J > 2$ will also be split into triplets. Figure 7 shows the energy levels for $J = 0, 1$, and 2.

HC¹⁴N and C¹⁷O Hyperfine Energy Levels

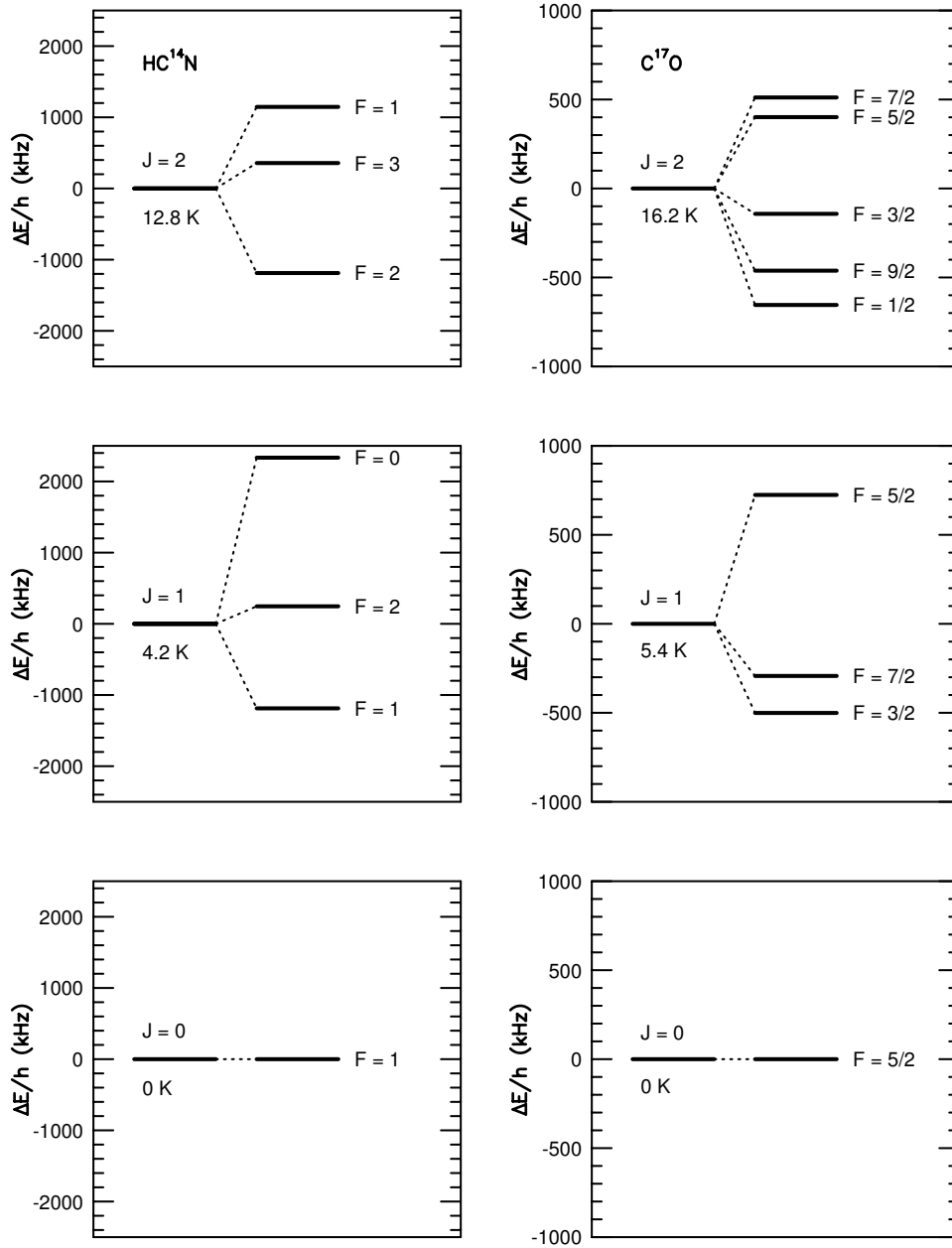


Fig. 7.— The hyperfine energy level structure of HCN and C¹⁷O for J = 0, 1, and 2. The vertical axis is the shift in energy ($\Delta E = E_Q + E_M$) in kHz. Note the vertical scale is different for HCN and C¹⁷O.

A good example of $I = 5/2$ hyperfine structure is $C^{17}O$. Using equations (10), we see that the $J = 0$ level remains unsplit ($F = 5/2$), the $J = 1$ level splits into a triplet ($F = 7/2, 5/2, 3/2$), the $J = 2$ level splits into 5 hyperfine levels ($F = 9/2, 7/2, 5/2, 3/2, 1/2$), and the $J = 3$ level into 6 hyperfine levels ($F = 11/2, 9/2, 7/2, 5/2, 3/2, 1/2$). The selection rule allows three hyperfine transitions from $J = 1 \rightarrow 0$, nine hyperfine transitions from $J = 2 \rightarrow 1$, and 14 hyperfine transitions from $J = 3 \rightarrow 2$. All of the transitions for $J = 2 \rightarrow 1$ are listed in Table 3 and the energy levels for $J = 1$ and $J = 2$ are shown in Figure 7. All levels with $J \geq 3$ will be split into 6 hyperfine levels. Figure 7 shows the $C^{17}O$ spectrum for $J = 1 \rightarrow 0$ and $J = 2 \rightarrow 1$ using the techniques discussed in Section 2.2.2.

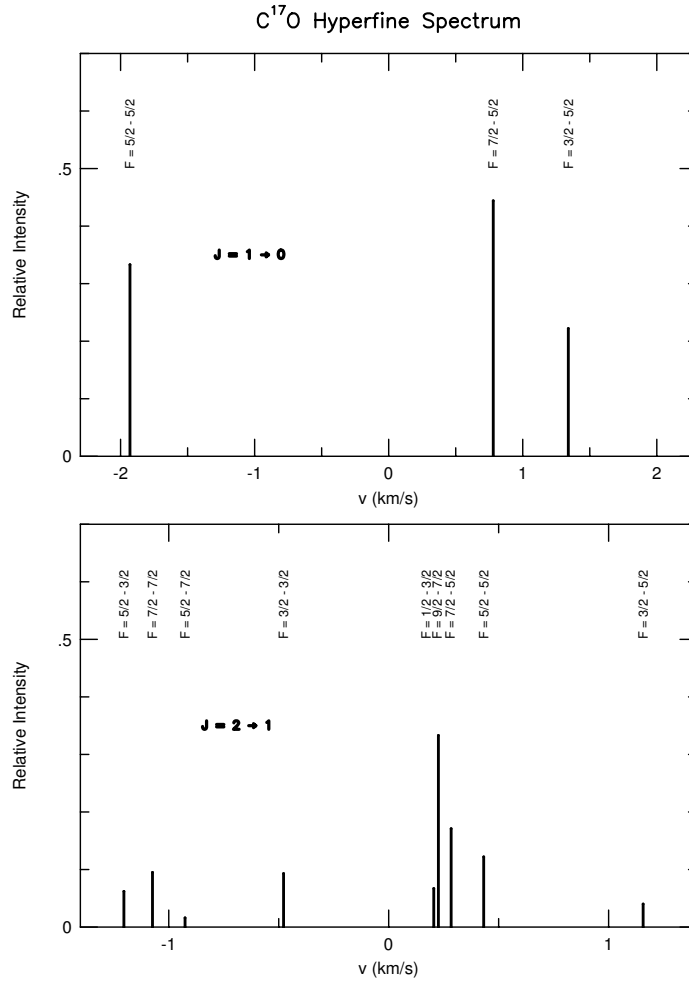


Fig. 8.— The hyperfine spectrum of $C^{17}O$ $J = 2 \rightarrow 1$ and $J = 1 \rightarrow 0$. The vertical axis is relative intensity and the horizontal axis is velocity (km/s) in the rest frame of the molecule.

2.2.2. Frequency of Hyperfine Transitions and Relative Strength

The energy shifts due to electric quadrupole and magnetic hyperfine coupling are treated as perturbations of the rotational Hamiltonian. First I will treat the electric quadrupole coupling, then the magnetic hyperfine coupling. The following treatment is a distilled version of Ramsey (1953), Townes & Schawlow 1975 (TS75), and Gordon & Cook 1984 (GC84).

To first order, we can write the perturbation due to an electric quadrupole moment as

$$\Delta E_Q = \langle I, J, F, M_F | \hat{H}_Q | I, J, F, M_F \rangle, \quad (11)$$

where we have assumed that J is a good quantum number (i.e. that \hat{H}_Q is diagonal. In reality, \hat{H}_Q is not exactly diagonal and J is perturbed by nuclear interactions. But, I will show later that second order effects are negligible). To solve Equation (11), we need to find an expression for the electric quadrupole Hamiltonian. Both TS75 and GC84 contain lucid derivations. The final solution for a linear diatomic molecule is given by

$$\hat{H}_Q = -eQq \frac{J \left[3(\vec{I} \cdot \vec{J})^2 + \frac{3}{2}\vec{I} \cdot \vec{J} - \vec{I}^2 \vec{J}^2 \right]}{2I(2I-1)(2J-1)J(2J+3)}, \quad (12)$$

where e is the charge, Q is the electric quadrupole moment, and q describes the magnitude of the component of the electric quadrupole tensor ($q_{xx} = q_{yy} = -\frac{1}{2}q_{zz} = q$ because the field gradient at the nucleus is symmetric about the bond axis). By using Equation (9) we can solve for the energy perturbations by evaluating the eigenvalues for $(\vec{I} \cdot \vec{J})^2$, $\vec{I} \cdot \vec{J}$, and $\vec{I}^2 \vec{J}^2$,

$$\langle I, J, F | \vec{I} \cdot \vec{J} | I, J, F \rangle = \frac{1}{2} [F(F+1) - I(I+1) - J(J+1)] \equiv \frac{1}{2}C \quad (13)$$

$$\langle I, J, F | (\vec{I} \cdot \vec{J})^2 | I, J, F \rangle = \frac{1}{4}C^2 \quad (14)$$

$$\langle I, J, F | \vec{I}^2 \vec{J}^2 | I, J, F \rangle = I(I+1)J(J+1), \quad (15)$$

(N.B. even though the vector notation is used, $\vec{I} \cdot \vec{J}$ etc. are operators). Plugging in the eigenvalues, we find

$$\Delta E_Q = -eQq \frac{\left[\frac{3}{4}C(C+1) - I(I+1)J(J+1) \right]}{2I(2I-1)(2J-1)(2J+3)}, \quad (16)$$

where $-eQq$ is the quadrupole coupling constant and the remaining expression on the right is Casimer's function (sometimes denoted $Y(I, J, F)$).

As mentioned above, the Hamiltonian, \hat{H}_Q , is not exactly diagonal due to perturbations of the rotational angular momentum, J . As a result, second order perturbation theory could be used to obtain a more accurate energy shift. However, TS75 show that the magnitude of this effect is of the order $\frac{eQq}{\nu}$. Second order perturbations are typically 5 orders of magnitude smaller than electric quadrupole coupling and 3 orders of magnitude smaller than magnetic hyperfine interactions. First order perturbation theory is more than sufficient for the current resolution of submm spectrometers. Second order corrections can be found in TS75 Appendix 2.

As with nuclear electric quadrupole coupling, there is coupling between the nuclear magnetic moment and the magnetic field generated by molecular rotation. We can calculate the magnetic coupling energy with

$$\Delta E_M = \langle I, J, F, M_F | \hat{H}_M | I, J, F, M_F \rangle, \quad (17)$$

where $\hat{H}_M = -\vec{\mu} \cdot \vec{H}_{eff}$ and $\mu \sim \vec{I}$ is the nuclear magnetic moment and $\vec{H}_{eff} \sim \vec{J}$ is the effective generated magnetic field. For a linear dipole molecule, the magnetic coupling Hamiltonian can be reduced to (again, see TS75 and GC84)

$$\hat{H}_M = C_I \vec{I} \cdot \vec{J}, \quad (18)$$

where C_I is the nuclear magnetic coupling constant (the only non-zero element of the nuclear magnetic coupling tensor, $C_{xx} = C_{yy} = C_I$). Plugging in the eigenvalue of $\vec{I} \cdot \vec{J}$ from Equation(13), we find the energy perturbations due to magnetic coupling are

$$\Delta E_M = \frac{C_I}{2} [F(F+1) - I(I+1) - J(J+1)]. \quad (19)$$

The total frequency shifts relative to the unshifted frequency due to electric quadrupole and magnetic hyperfine coupling are given by

$$\nu_{if} - \nu_{unsplit} = \frac{\Delta E_i - \Delta E_f}{h}, \quad (20)$$

where i is the initial F level, f is the final F level, and $\Delta E = E_Q + E_M$.

The relative strengths can be calculated by using irreducible tensor methods (see Gordy & Cook (1984) Chapter 15). We define the relative strength such that the sum of the relative strength, s, of all transitions from $F' \rightarrow F$ for a given $J' \rightarrow J$ are equal to one (see Rudolph 1968):

$$\sum_{F'F} s(IJ'F' \rightarrow IJF) = 1. \quad (21)$$

The relative line strengths are calculated in terms of a 6 - j symbol,

$$s(IJ'F' \rightarrow IJF) = \frac{(2F+1)(2F'+1)}{(2I+1)} \left\{ \begin{array}{ccc} I & F' & J' \\ 1 & J & F \end{array} \right\}^2. \quad (22)$$

With the aid of 6 - j Tables (Edmonds 1974), and the property that 6 - j symbols are invariant with permutation of the columns, we find the appropriate 6 - j symbol for each transition:

$$\left\{ \begin{array}{ccc} I & F & J \\ 1 & J-1 & F-1 \end{array} \right\}^2 = \frac{a(a+1)(a-2I-1)(a-2I)}{(2F-1)2F(2F+1)(2J-1)2J(2J+1)} \quad (23)$$

$$\left\{ \begin{array}{ccc} I & F & J \\ 1 & J-1 & F \end{array} \right\}^2 = \frac{2(a+1)(a-2I)(a-2F)(a-2J+1)}{2F(2F+1)(2F+2)(2J-1)2J(2J+1)} \quad (24)$$

$$\left\{ \begin{array}{ccc} I & F & J \\ 1 & J-1 & F+1 \end{array} \right\}^2 = \frac{(a-2F-1)(a-2F)(a-2J+1)(a-2J+2)}{(2F+1)(2F+2)(2F+3)(2J-1)2J(2J+1)}, \quad (25)$$

where $a = F + J + I$.

2.2.3. Multiple Coupling Nuclei

There are a few important linear molecules with multiple coupling nuclei. Important astrophysical examples include N_2H^+ , N_2D^+ , and DCN. In general, there are two coupling schemes for multiple coupling nuclei. For hyperfine coupling when one nucleus has a much stronger coupling strength than the next nucleus (e.g. $(eQq)_1 \gg (eQq)_2$, etc.) we use the basis $|JF_1F_2 \cdots F \rangle$ where

$$\begin{aligned}\vec{F}_1 &= \vec{I}_1 + \vec{J} \\ \vec{F}_2 &= \vec{I}_2 + \vec{F}_1 \\ &\vdots \\ \vec{F} &= \vec{I}_n + \vec{F}_{n-1}\end{aligned}\tag{26}$$

where I_i is the spin of the i^{th} nucleus and $F_i = F_i + I_i, F_i + I_i - 1, \dots, |F_i - I_i|$ for each hyperfine quantum number. For hyperfine coupling when the nuclei have equal coupling strength we use the basis $|J\mathcal{I}_2\mathcal{I}_3 \cdots \mathcal{I}F \rangle$ where

$$\begin{aligned}\vec{\mathcal{I}}_2 &= \vec{I}_1 + \vec{I}_2 \\ \vec{\mathcal{I}}_3 &= \vec{\mathcal{I}}_2 + \vec{I}_3 \\ &\vdots \\ \vec{\mathcal{I}} &= \vec{\mathcal{I}}_{n-1} + \vec{I}_n \\ \vec{F} &= \vec{\mathcal{I}} + \vec{J}.\end{aligned}\tag{27}$$

Both N_2H^+ and N_2D^+ are examples of molecules with unequal coupling strengths and therefore use the first coupling scheme. The second coupling scheme is more important in molecules with higher degrees of symmetry (e.g. D_2O where the hyperfine coupling strengths of the two D nuclei are identical). I shall explain the observed hyperfine structure for N_2H^+ .

The hyperfine energy levels for N_2H^+ can be formed by using the Clebsch-Gordan series due to the outer nitrogen (F_1) and due to the inner nitrogen (F). The hyperfine coupling constants are: $(eQq)_1 = -5.6902 \pm 0.0021$ MHz, $(eQq)_2 = -1.3586 \pm 0.0038$ MHz, $C_1 = 11.8 \pm 0.4$ kHz, $C_2 = 8.7 \pm 0.6$ kHz (Caselli, Myers, & Thaddeus 1995). For the $J=0$ level, the outer nitrogen results in only one energy level $F_1 = 1$ (see Figure 8). The inner nitrogen further splits the $F_1 = 1$ level into three energy levels: $F=0, 1, 2$. For the $J=1$ level, the outer nitrogen coupling results in the triplet: $F_1 = 0, 1, 2$. The inner nitrogen splits the $F_1 = 2$ level into a triplet ($F=1, 2, 3$), the $F_1 = 1$ level into a triplet ($F=0, 1, 2$), and the $F_1 = 0$ level does not split and becomes $F=1$. Thus, the $J=1$ level is split into seven hyperfine level and the $J=0$ is split into three energy levels when coupling from both nuclei are included. If we continue to higher J levels, we will see that each level from $J=2$ and higher is split into nine hyperfine levels.

Selection rules are similar to the single coupling case: $\Delta F_1 = 0, \pm 1$, $\Delta F = 0, \pm 1$ with $0 \not\rightarrow 0$, $\Delta J = \pm 1$. Therefore, in the $J=1 \rightarrow 0$ transitions of N_2H^+ and N_2D^+ , there are fifteen allowed

transitions. However, since the $J=0$ splitting is very small, only seven transitions from the seven hyperfine $J=1$ levels are observed (Figure 9). Recently the hyperfine structure of N_2H^+ and N_2D^+ up to the $J=3 \rightarrow 2$ transition has been calculated and observed (Gerin et al. 2001).

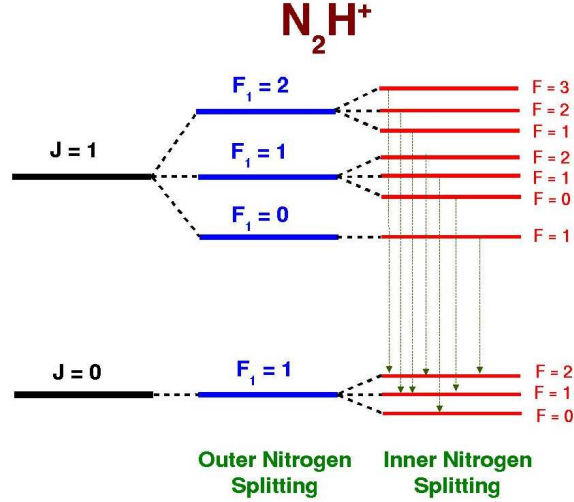


Fig. 9.— Diagrammatic representation of the hyperfine energy levels for N_2H^+ $J=1 \rightarrow 0$. The $J=0$ level is not actually split into separate energy levels. The seven observed transitions from the seven upper hyperfine levels are shown.

2.2.4. Multiple Coupling Nuclei - Energy Levels & Strength

Calculating the hyperfine energy levels for multiple coupling nuclei is more complicated. Irreducible tensor methods provide elegant and tractable techniques and are used in all modern papers (see The Journal of Molecular Spectroscopy, etc.). The hyperfine Hamiltonian for n coupling nuclei can be expressed as as

$$H_{hfs} = \sum_{i=1}^n \left[\mathbf{V}^{(2)}(i) \cdot \mathbf{Q}^{(2)}(i) + \mathbf{m}^{(1)}(i) \cdot \boldsymbol{\mu}^{(1)}(i) \right] + H_{spin-spin} \quad (28)$$

where $\mathbf{V}^{(2)}(i)$ and $\mathbf{Q}^{(2)}(i)$ are the second rank electric field gradient and electric quadrupole spherical tensors at the i^{th} nucleus, $\mathbf{m}^{(1)}(i) \cdot \boldsymbol{\mu}^{(1)}(i)$ is the magnetic dipole interaction in spherical tensor notation, and $H_{spin-spin}$ is the hyperfine Hamiltonian due to spin-spin interactions between nuclei and is usually negligible for astrophysical spectroscopy (the interaction for 2 nuclei is given by $H_{spin-spin} = -\sqrt{5/2}[\mathbf{D}_{21}^{(2)} \times \mathbf{I}_2^{(1)}]^{(1)} \cdot \mathbf{I}_1^{(1)}$, where $\mathbf{D}_{21}^{(2)}$ is the second rank spin coupling spherical tensor - see GC84 section 15.5). Expressions for the matrix elements of $\mathbf{V}^{(2)}(i) \cdot \mathbf{Q}^{(2)}(i)$ and $\mathbf{m}^{(1)}(i) \cdot \boldsymbol{\mu}^{(1)}(i)$ for the two coupling schemes can be found in Chapter 15 of GC84 (e.g. equations 15.102, 15.103, 15.115, & 15.116). The matrix element for the electric quadrupole interaction and the magnetic

dipole interaction for two unequal coupling nuclei in a linear molecule is given by (see GC84)

$$\begin{aligned} \Delta E_Q &= \frac{(-1)^t (eQq)_1 J}{2(2J+3) \begin{pmatrix} J & 2 & J \\ J & 0 & -J \end{pmatrix} \begin{pmatrix} I_1 & 2 & I_1 \\ -I_1 & 0 & I_1 \end{pmatrix}} \begin{Bmatrix} F_1 & I_1 & J \\ 2 & J & I_1 \end{Bmatrix} \\ &+ \frac{(-1)^r (eQq)_2 J (2F_1 + 1)}{2(2J+3) \begin{pmatrix} J & 2 & J \\ J & 0 & -J \end{pmatrix} \begin{pmatrix} I_2 & 2 & I_2 \\ -I_2 & 0 & I_2 \end{pmatrix}} \\ &\times \begin{Bmatrix} I_2 & F_1 & J \\ 2 & J & F_1 \end{Bmatrix} \begin{Bmatrix} F & I_2 & F_1 \\ 2 & F_1 & I_2 \end{Bmatrix} \end{aligned} \quad (29)$$

$$\begin{aligned} \Delta E_M &= (-1)^t C_1 [J(J+1)(2J+1)]^{1/2} [I_1(I_1+1)(2I_1+1)]^{1/2} \begin{Bmatrix} F_1 & I_1 & J \\ 1 & J & I_1 \end{Bmatrix} \\ &+ (-1)^{r+1} C_2 (2F_1 + 1) [J(J+1)(2J+1)]^{1/2} [I_2(I_2+1)(2I_2+1)]^{1/2} \\ &\times \begin{Bmatrix} I_1 & F_1 & J \\ 1 & J & F_1 \end{Bmatrix} \begin{Bmatrix} F & I_2 & F_1 \\ 1 & F_1 & I_1 \end{Bmatrix} \end{aligned} \quad (30)$$

where $t = J + I_1 + F_1$ and $r = J + I_1 + I_2 + 2F_1 + F$. These equations represent the first order perturbation to the energy levels for unequal coupling nuclei. For equal or nearly equal coupling nuclei, a similar set of expressions based on the coupling scheme given in equation (28) and (29) is derived (see GC84). If we ignore the second term in ΔE_Q and ΔE_M , then we recover the same expressions derived section 2.2.2 for a single coupling nucleus. We extend the method used to calculate the relative strengths to find the relative strength for two coupling nuclei (electric dipole transitions)

$$\begin{aligned} s(J'F_1'F' \rightarrow JF_1F) &= \frac{(2F_1' + 1)(2F_1 + 1)(2F' + 1)(2F + 1)}{(2I_1 + 1)(2I_2 + 1)} \\ &\times \begin{Bmatrix} I_1 & F_1' & J' \\ 1 & J & F_1 \end{Bmatrix}^2 \begin{Bmatrix} I_2 & F' & F_1' \\ 1 & F_1 & F \end{Bmatrix}^2. \end{aligned} \quad (31)$$

The 3j and 6j symbols needed in equations (29 - 31) can be found in Edmonds (1974).

3. Symmetric Top Molecules

3.1. Rotational Spectrum

Symmetric top molecules are molecules that have a symmetry axis with the two principle moments of Inertia equal. We can define a coordinate system (called the body axes), (x, y, z) , with z along the molecular symmetry axis. In this coordinate frame, the moment of Inertia tensor is diagonal and the moments of Inertia about the two axes perpendicular to the symmetry axis are equal, $I_x = I_y$. The designations A, B, and C are traditionally used instead of x, y, z . Therefore, I_x and $I_y \rightarrow I_B$ and $I_z \rightarrow I_A$ or $I_z \rightarrow I_C$ depending on whether I_z is greater than (prolate) or less than I_B (oblate; see Figure 10). Therefore, symmetric top molecules are classified into three categories: spherical tops with $I_A = I_B = I_C$; prolate symmetric tops with $I_A < I_B$; and oblate symmetric tops with $I_C > I_B$. Linear molecules are just a special case of symmetric tops in which $I_B = 0$. It should be noted that the body coordinates axes, (x, y, z) , are not fixed in space (they precess) and should not be confused with the fixed space axes (X, Y, Z) .

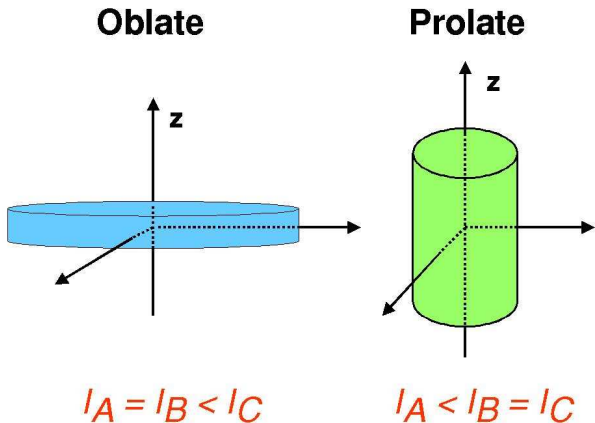


Fig. 10.— Oblate and prolate symmetric tops.

In the body coordinate frame of the molecule, we find the total kinetic energy of rotation to be (see equation (2)),

$$T = \frac{\vec{J}_x^2}{2I_x} + \frac{\vec{J}_y^2}{2I_y} + \frac{\vec{J}_z^2}{2I_z}, \quad (32)$$

and the total angular momentum is

$$\vec{J}^2 = \vec{J}_x^2 + \vec{J}_y^2 + \vec{J}_z^2. \quad (33)$$

In the classical symmetric top, the total angular momentum, \vec{J} , and its projection on the symmetry axis in the body frame, \vec{J}_z , are constants of the motion. In quantum mechanics, both of these quantities are observable (i.e. $[\hat{J}_z, \hat{H}_{rot}] = 0$ and $[\hat{J}^2, \hat{J}_z] = 0$). We can rewrite the kinetic energy in terms of \hat{J} and \hat{J}_z by substituting equation (33) into (32) and changing to the A,B,C notation

(since most molecules observed are prolate, we will use that designation; for oblate molecules, then simply substitute $A \rightarrow C$)

$$T = \frac{J^2}{2I_B} + J_z^2 \left(\frac{1}{2I_A} - \frac{1}{2I_B} \right). \quad (34)$$

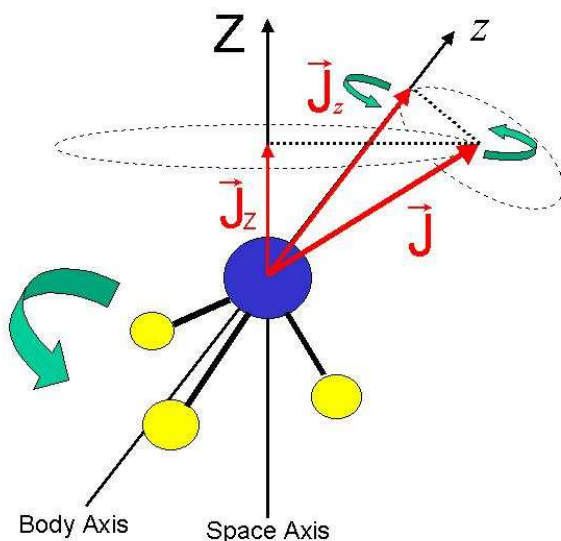


Fig. 11.— The vector model for a symmetric-top molecule.

Classically, the total angular momentum is fixed in space and \vec{J}_z precesses about \vec{J} . However, due to the uncertainty principle, we cannot measure the total angular momentum's magnitude and direction in space simultaneously. We can only measure the total magnitude of the angular momentum squared and the projection of the total angular momentum on a fixed space axis, Z . Thus, there are 2 projections of the total angular momentum that are good quantum numbers, the projection on the space axis, \vec{J}_Z and the projection on the molecular body symmetry axis, \vec{J}_z (see Figure 8). The eigenvalues are found to be

$$\hat{J}^2 \Psi = \frac{h^2}{4\pi^2} J(J+1) \Psi \quad (35)$$

$$\hat{J}_Z \Psi = \frac{h}{2\pi} M_J \Psi \quad (36)$$

$$\hat{J}_z \Psi = \frac{h}{2\pi} K \Psi, \quad (37)$$

where K is the quantum number of the projection on the molecular symmetry axis and the wavefunction is given by $\Psi = |J, K, M_J\rangle$ in Dirac notation.

Since K is a projection of \vec{J} , K can take on the values $K = -J, -J+1, \dots, J-1, J$. K values at $\pm J, \pm(J-1)$, etc. are degenerate unless an asymmetry splits them (as we will see in asymmetric molecules). The energy of a symmetric top is then found by substituting the eigenvalues into the

the rotational Hamiltonian to give

$$E = \frac{\hbar^2 J(J+1)}{8\pi^2 I_B^2} + K^2 \left(\frac{\hbar^2}{8\pi^2 I_A} - \frac{\hbar^2}{8\pi^2 I_B} \right) = \hbar B J(J+1) + \hbar K^2 (A - B), \quad (38)$$

where $A = \frac{\hbar^2}{8\pi^2 I_A}$ and $B = \frac{\hbar^2}{8\pi^2 I_B}$ are now the rotational constants (in Dirac notation $E = \langle J, K, M_J | \hat{H}_{rot} | J, K, M_J \rangle$). Selection rules stipulate that $\Delta J = 0, \pm 1$ and $\Delta K = 0$. Note that $\Delta J = 0$ is now allowed (since $\pm K$ are degenerate, each J_K level has both symmetric and anti-symmetric degenerate levels). However, if we try and calculate the frequency of a transition from $J+1, K \rightarrow J, K$, we find that $\nu_{J+1, K \rightarrow J, K} = \hbar B (J+1)$ and the K dependence cancels out! In the rigid rotor approximation, transitions for different K levels are not resolved! But, the rigid rotor is no longer a good approximation and we must include effects such as centrifugal distortion to calculate the energy levels J_K and resolve transitions in different K ladders. For details, see TS75 and GC84.

A good example of a prolate symmetric top molecule is methyl acetylene (CH_3CCH). The first three K ladders of the methyl acetylene energy level diagram are shown in Figure 12. The energy levels are organized by the K quantum number since transition between different K are forbidden for electric dipole transitions. Notice that the lowest J level in each K ladder is $J=K$. Also, the energy of the lowest J level in each K ladder increases quadratically above the ground state energy (as it does for the linear molecule). Transitions in different K ladders for the same $J+1 \rightarrow J$ occur closely spaced in frequency. For instance, notice that the frequency of the $J = 3 \rightarrow 2$ transition for different K ladders are all near 51.27 GHz. This means that symmetric top molecules provide a very rich spectrum in which many transition are closely spaced in frequency for a given $J+1 \rightarrow J$.

EXAMPLE:

The first 4 K -ladder transitions of the $J = 13 \rightarrow 12$ transitions of CH_3CCH lie within 39 MHz of each other:

$13_0 \rightarrow 12_0$ 222.1669700 GHz
 $13_1 \rightarrow 12_1$ 222.1627287 GHz
 $13_2 \rightarrow 12_2$ 222.1500084 GHz
 $13_3 \rightarrow 12_3$ 222.1288080 GHz

By choosing a central frequency, such as 222.147889 GHz, all four transitions can easily be observed simultaneously with a 50 MHz high resolution spectrometer.

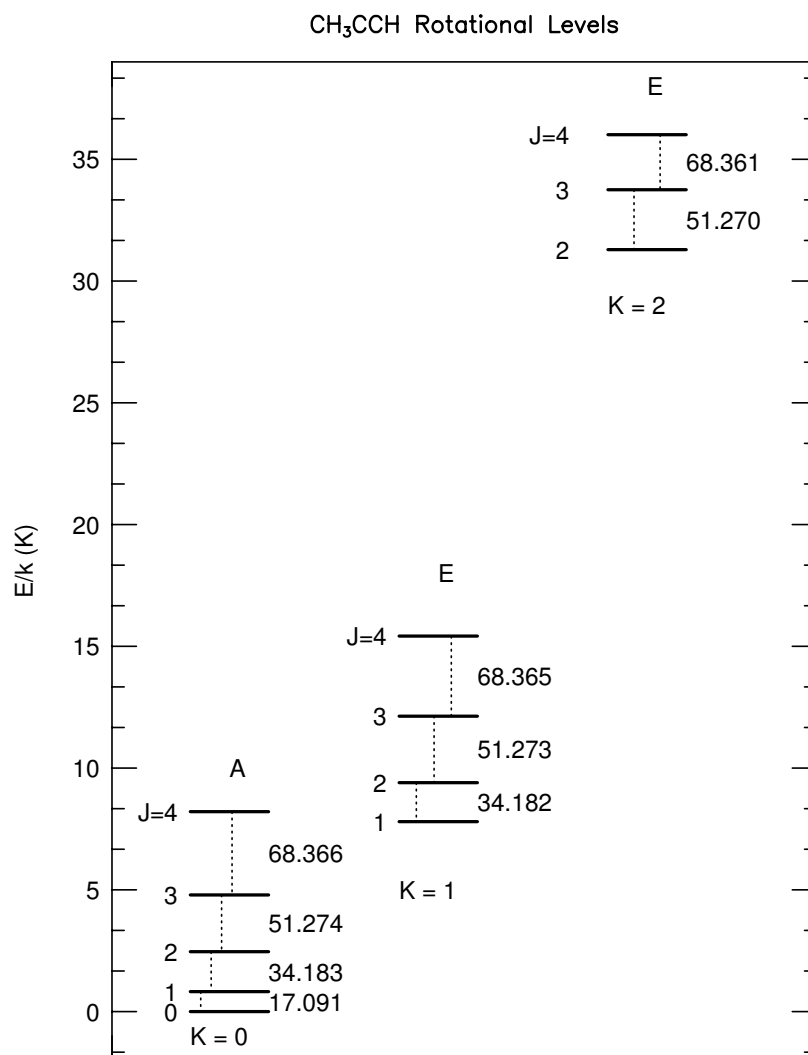


Fig. 12.— The rotational energy level diagram for CH₃CCH. The vertical axis is energy in units of K. The first three K ladders are shown up to J=4. The A and E above each K ladder refers to the C_{3v} symmetry species. All transition frequencies are in units of GHz and are displayed accurately.

3.2. Inversion Splitting

A few astrophysically important molecules (NH_3 , H_3O^+) can undergo inversion that splits each of the rotational levels into 2 separate levels. The best example is NH_3 . The N nucleus can tunnel through the plane of the 3 H nuclei, oscillating between two equilibrium positions. Figure 13 shows the potential energy curve for the oscillating nitrogen. If we denote the wavefunction by Ψ_L and Ψ_R when the nitrogen is in the left and right potential energy minima, then the total wavefunction can be formed from symmetric and antisymmetric combinations of these two wavefunctions,

$$\Psi_+ = \frac{1}{\sqrt{2}} (\Psi_L + \Psi_R) \quad (39)$$

$$\Psi_- = \frac{1}{\sqrt{2}} (\Psi_L - \Psi_R). \quad (40)$$

Therefore, each rotational level is split into 2 levels denoted by the symmetry of the inversion level (+ or -).

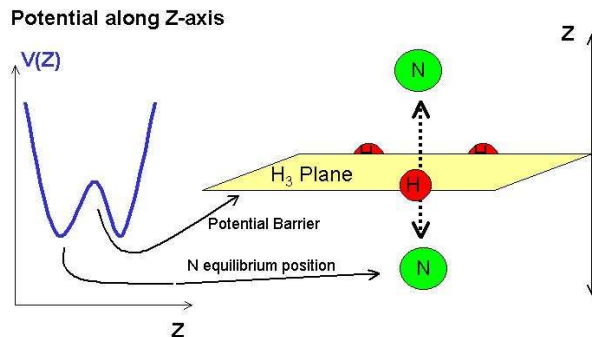


Fig. 13.— Inversion of the Nitrogen in ammonia. The potential energy curve along the Z-axis is shown to the left. In the fundamental inversion transition, the Nitrogen tunnels through the H_3 potential barrier at 23.6 GHz.

Selection rules stipulate that the parity must change for electric dipole transitions; therefore, transitions must change inversion level symmetry (+ \rightarrow -). The potential barrier must be low for inversions to occur. In practice, only a few molecules have observable inversion levels (e.g. NH_3 , NH_2D). When the potential barrier becomes infinite in height, the inversion levels are degenerate. This is the case for CH_3CCH shown in Figure 12. The energy level diagram for NH_3 is shown in Figure 14. Transition between inversion levels for the same J_K are typically in the cm part of the spectrum (i.e. the $\text{inv}(1,1)$ transition for NH_3 is at 23.694 GHz). Because NH_3 has 3 H nuclei, the overall wavefunction obeys Fermi-Dirac statistics. Spin statistics eliminate 1 inversion level for the $K = 0$ ladder (for details see §3.4 of TS75). The rotational transitions with $\Delta J = -1$ occur in the submm and far-infrared part of the spectrum.

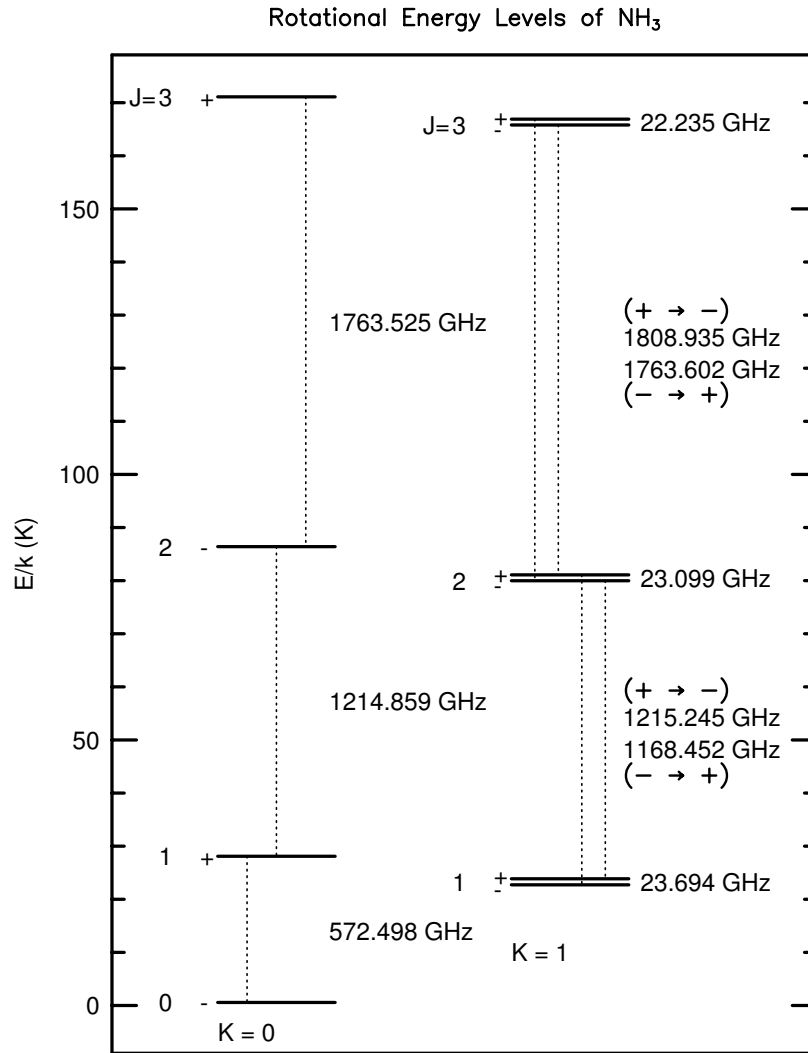


Fig. 14.— The rotational energy level diagram for the oblate symmetric top NH₃. The vertical axis is energy above ground in K. All energy levels are displayed accurately. Only the first two K ladders up to J=3 are shown. The + and - refer to the symmetry of the inversion level. Effects of hyperfine splitting are not shown.

3.3. Hyperfine Structure - Symmetric Top

Since nearly all astrophysically important symmetric top molecules have a pyramidal -H₃ structure (C_{3v} symmetry, or unchanged by rotation of 120°), each molecule exhibits a rich hyperfine pattern. As in the linear case, the hyperfine splitting is dominated by electric quadrupole coupling. In the case of CH₃CN and NH₃, the N nucleus dominates the hyperfine splitting. The equations used to calculate the energy shifts remain the same for symmetric top molecules with the coupling nucleus along the symmetry axis, but with the electric field gradient tensor multiplied by an additional term accounting for the off axis nuclei

$$q_J = q \frac{J}{(2J + 3)} \left[\frac{3K^2}{J(J + 1)} - 1 \right]. \quad (41)$$

The term in brackets would be multiplied into equations (16) and (29). The hyperfine splitting occurs for each J_K rotational level. I shall describe the hyperfine levels for two common symmetric tops, CH₃CN (ignoring -H₃ coupling) and NH₃ (including -H₃ coupling).

The hyperfine structure of symmetric top molecules is analogous to the linear case. A Clebsch-Gordon series is formed for every rotational level, J_K . In the case of CH₃CN, the electric quadrupole coupling due to the N splits each rotational level with $J \geq 1$ into a triplet. Using the usual selection rules, $\Delta F = 0, \pm 1$, there are 6 allowed transitions (see Figure 15).

In general, the splitting due to H₃ is much less than the N. However, in the case of NH₃ both must be taken into account. Figure 16 shows the hyperfine splitting due to the N and due to H₃. Since the three H nuclei are in symmetric positions in the molecule, they contribute equally to hyperfine splitting. The 3 H spins are combined into a single quantum number, I_H . Therefore, the quantum numbers for NH₃ follow the hyperfine splitting scheme for 2 coupling nuclei ($J F_1 F$).

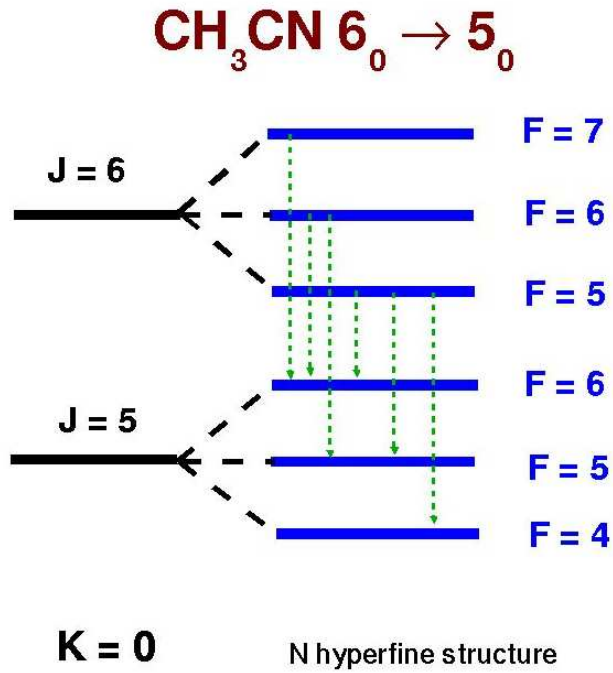


Fig. 15.— Diagrammatic representation of the hyperfine splitting of the $J_K = 6_0$ and 5_0 energy levels of CH_3CN . The electric dipole allowed transitions are shown in green and range from 110.3820283 GHz to 110.3852193 GHz (JPL line catalog). Actual hyperfine shifts of the energy level are not shown.

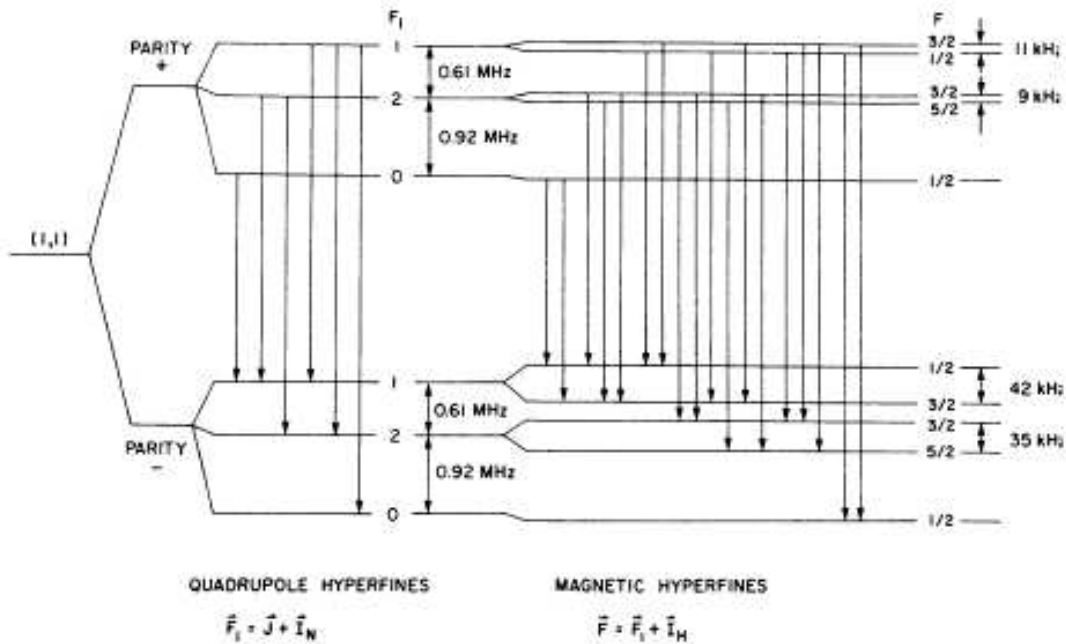


Fig. 15.— Hyperfine splitting in NH_3 . Figure was pinched from Ho & Townes 1983, ARA&A.

4. Asymmetric Top Molecules

4.1. Rotational Spectrum

Asymmetric top molecules have none of the three principle moments of Inertia of the molecule equal. Typically, we write the moment of Inertia in the order, $I_A < I_B < I_C$. Asymmetric tops are classified into prolate asymmetric tops ($I_B \rightarrow I_C$) and oblate asymmetric tops ($I_B \rightarrow I_A$). We can define the degree of asymmetry using Ray’s asymmetry parameter,

$$\kappa = \frac{2B - A - C}{A - C}, \quad (42)$$

where $A = \frac{\hbar^2}{8\pi^2 I_A}$, $B = \frac{\hbar^2}{8\pi^2 I_B}$, and $C = \frac{\hbar^2}{8\pi^2 I_C}$. A molecule that is the most asymmetric would have $\kappa = 0$. A prolate asymmetric top has $\kappa \rightarrow -1$ and an oblate asymmetric top has $\kappa \rightarrow +1$. Table 5 lists the molecular parameters for a few asymmetric top molecules.

Since there is no longer a symmetry axis in the molecule, there is no longer an internal component to the angular momentum that is a constant of the motion (as J_z was in the symmetric top). Now we find $[\hat{J}_z, \hat{H}_{rot}] \neq 0$ and $[\hat{J}_z, \hat{J}^2] \neq 0$. In fact, expressions for the energy levels are found in term of expansions (for instance, using linear combinations of symmetric top wavefunction, $|JKM_J\rangle$). Details can be found in TS75 and GC84.

There is still a convenient way to describe the energy levels of an asymmetric molecule. In the symmetric top, we could not distinguish between degenerate K levels ($K = \pm J, \pm(J-1), \dots$). Now, due to the asymmetry, we can now distinguish between different projections of \vec{J} on an internal axis in the molecule. The quantum numbers are given as $J_{K_{-1}K_{+1}}$ where K_{-1} is the projection of \vec{J} in the limit that the molecules is prolate and K_{+1} is the projection of \vec{J} in the limit that the molecule is oblate. Sometimes, K_{+1} and K_{-1} are also denoted by K_A and K_C . $K_{\pm 1}$ are **NOT** good quantum numbers, they are merely used to keep track of the order of energy levels. They are most useful when a molecule is very nearly prolate or very nearly oblate. In the prolate case, the energy levels would be ordered: $0_{00}, 1_{01}, 1_{11}, 1_{10}, 2_{02}, 2_{12}, 2_{11}, 2_{21}, 2_{20}, \dots$ increasing in energy above ground (0_{00}). In the nearly oblate case we find: $0_{00}, 1_{10}, 1_{11}, 1_{01}, 2_{20}, 2_{21}, 2_{11}, 2_{12}, 2_{02}, \dots$ increasing in energy above ground (0_{00}). Notice the order of the levels are opposite for nearly prolate and nearly oblate molecules.

The selection rules for asymmetric tops depend on the symmetry properties of the total wavefunction (electric dipole transitions require a change of parity). The selection rule for J is the same as for the symmetric top: $\Delta J = 0, \pm 1$. The selection rules for ΔK_{-1} and ΔK_{+1} depend on whether K_{-1} or K_{+1} is even or odd. Table 6 lists the selection rules. For most astrophysical applications, the $\Delta K_{\pm 1} = \pm 2, \pm 3, \dots$ are highly unlikely. So, for a molecule with μ along the principle axis with the least moment of inertia (i.e. H_2CO , $\mu_A \neq 0$), transition between K_{-1} ladders are highly unlikely and $\Delta K_{+1} = \pm 1$. These transitions are sometimes called “a-type” transitions. For a more asymmetric molecule with μ along the principle axis with the intermediate moment of inertia (i.e. H_2O , $\mu_B \neq 0$), $\Delta K_{-1} = \pm 1$ and $\Delta K_{+1} = \pm 1$. These transitions are sometimes called “b-type”

transitions. For a molecule with μ along the principle axis with the greatest moment of inertia (i.e. NH_2D , $\mu_C \neq 0$), transitions between K_{+1} ladders are unlikely and $\Delta K_{-1} = \pm 1$. These transitions are sometimes called “c-type” transitions.

Figure 16 shows the energy level diagram for formaldehyde. Because H_2CO is a nearly prolate asymmetric top, transition between different K_{-1} ladders are highly forbidden. The transitions between the split J levels for $K_{-1} = 1$ occur at cm wavelengths (4.8 GHz, etc.). Transitions between different J levels are much higher in frequency, in the mm and submm part of the spectrum. Notice that transitions in different K_{-1} ladders for same $J+1 \rightarrow J$ occur at similar frequencies (e.g. $J=3 \rightarrow 2$ are near 220 GHz).

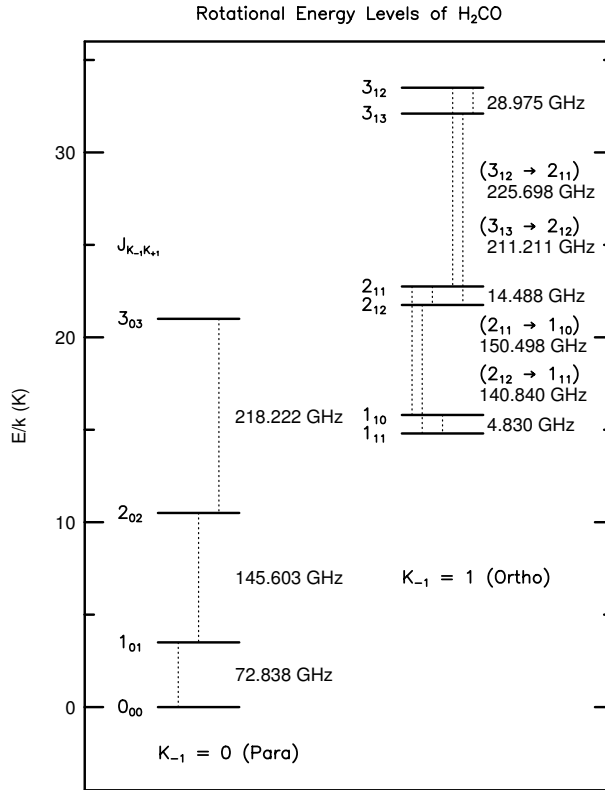


Fig. 16.— The rotational energy level diagram for H_2CO . The vertical axis is energy above ground in K . All energy levels are displayed accurately except the splitting between the 1_{10} 1_{11} and 2_{11} 2_{12} levels. Only the first two K_{-1} ladders up to $J=3$ are shown.

Water is a good example of a molecule that is intermediate between the prolate and oblate case. The dipole moment is aligned along the intermediate principle axis ($\mu_B \neq 0$). Therefore, transitions are allowed between K_{-1} and K_{+1} ladders. The energy level diagram is shown in Figure 17. The $1_{10} \rightarrow 1_{01}$ transition at 556.9 GHz was recently observed with SWAS, the Submillimeter Wave Astronomy Satellite.

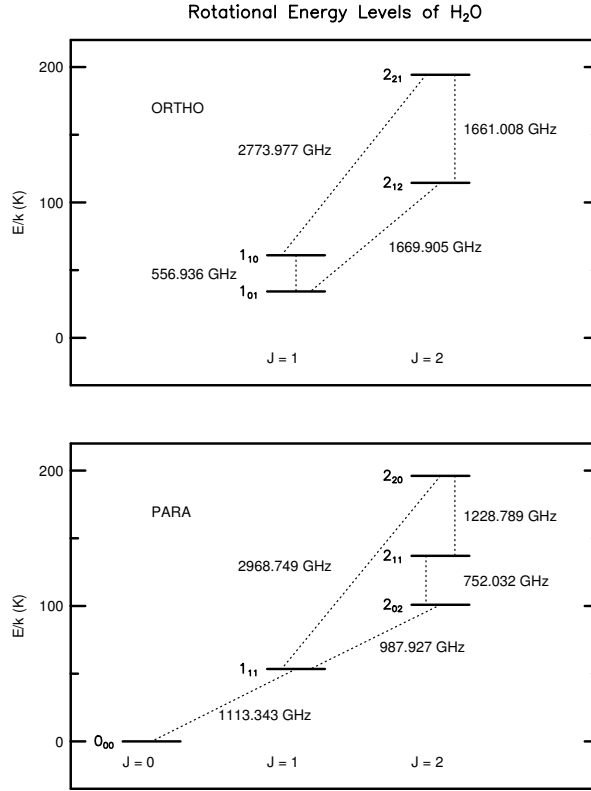


Fig. 17.— The rotational energy level diagram for H₂O. The vertical axis is energy above ground in K. All energy levels are displayed accurately. Since transitions between $K_{\pm 1}$ ladders are allowed, energy levels are organized by J. All energy levels up to $J = 2$ are shown.

Some more complicated asymmetric top molecules have dipole moments that are not aligned with the principle axes of the molecule. HNC0 is a good example of a planar molecule with both μ_A and $\mu_B \neq 0$. Therefore, selection rules indicate that $\Delta K_{-1} = 0, \pm 1$ and $\Delta K_{+1} = \pm 1$ (see Figure 18). Therefore, both “a-type” and “b-type” transitions are allowed.

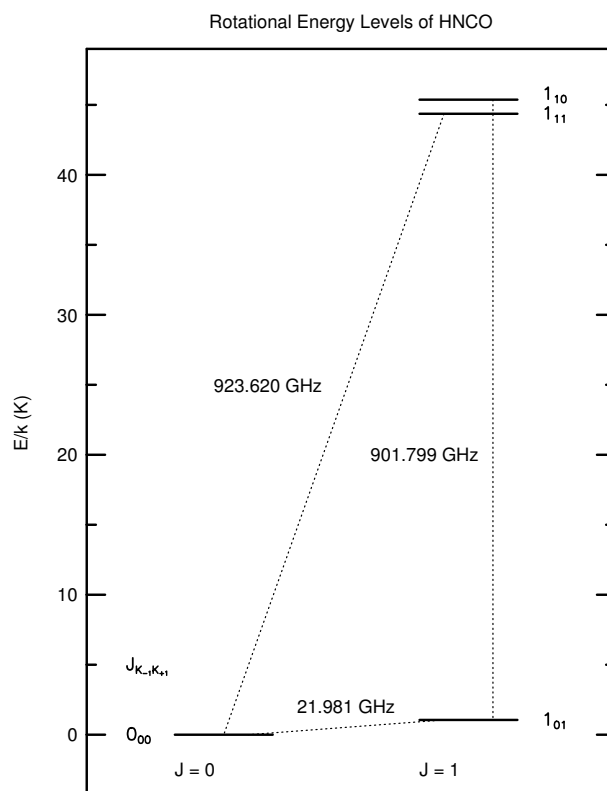


Fig. 18.— The rotational energy level diagram for HNC0. The vertical axis is energy above ground in K. All energy levels are displayed accurately except the 1_{10} and 1_{11} levels. Since transitions between $K_{\pm 1}$ ladders are allowed, energy levels are organized by J . All transition with frequencies greater than 1 GHz are shown. Hyperfine structure not shown.

4.2. Nuclear Spin Statistics - 2 Identical Nuclei

Many asymmetric molecules have 2 identical nuclei. The most common astrophysical cases are molecules that have C_{2v} symmetry, where the molecule is unchanged with a rotation of π about the symmetry axis and a reflection of π through the symmetry plane. Common examples of C_{2v} symmetric molecules are H_2CO , H_2O , and SO_2 . Nuclear spin statistics determine the statistical weights of energy levels and can cause levels to not exist (e.g. SO_2).

4.2.1. Ortho & Para - 2 H nuclei

The most common astrophysical case is a molecule with 2 H atoms and the other nuclei with spin 0. Since H has a spin of $\frac{1}{2}$, the overall wavefunction (given by equation (36)) has to obey Fermi-Dirac Statistics and be antisymmetric with respect to interchange of the identical nuclei (corresponding to a rotation of π about the symmetry axis for C_{2v} molecules). The total wavefunction can be written as the product of the electronic (Ψ_E), vibrational (Ψ_V), rotational ($\Psi_{J_{K_{-1}K_{+1}}}$) and nuclear wavefunctions (Ψ_N),

$$\Psi_{total} = \Psi_E \Psi_V \Psi_{J_{K_{-1}K_{+1}}} \Psi_N. \quad (43)$$

For 2 spin $\frac{1}{2}$ particles, there are four ways to arrange their spins, 3 symmetric combinations ($|\uparrow\uparrow\rangle$, $|\downarrow\downarrow\rangle$, $\frac{1}{\sqrt{2}}(|\uparrow\downarrow\rangle + |\downarrow\uparrow\rangle)$) and 1 antisymmetric combination ($\frac{1}{\sqrt{2}}(|\uparrow\downarrow\rangle - |\downarrow\uparrow\rangle)$). The symmetric case (ortho) has a statistical weight that is 3 times that of the antisymmetric case (para).

For a molecule in the $^1\Sigma$ electronic state and the ground vibrational state, the electronic and vibrational wavefunctions are symmetric. The nuclear wavefunction can be either symmetric (ortho) or antisymmetric (para). The total wavefunction must be antisymmetric. Therefore, to determine which rotational levels are ortho or para, we need to know the symmetry of the rotational wavefunction with respect to a rotation of π about the symmetry axis of the molecule (see Table 7). We can now see another powerful use of the $J_{K_{-1}K_{+1}}$ notation. The rotational symmetry can be determined by using Table 7, knowing along which principle axis the dipole moment is aligned (Table 5), and noting which $K_{\pm 1}$ are even and odd.

In the previous section we considered H_2CO . Formaldehyde has its dipole moment aligned with the principle axis of least moment of Inertia ($\mu_A \neq 0$). Therefore, Table 7 tells us that $K_{-1}K_{+1}$ that are ee and eo have symmetric rotational wavefunctions. Since Ψ_{total} must be antisymmetric, then the nuclear wavefunction must be antisymmetric (para). So, all $K_{-1}K_{+1}$ that are ee and eo are para- H_2CO . The $K_{-1} = 0, 2, 4, \dots$ ladders satisfy this criteria and are therefore para- H_2CO . Table 7 also shows that $K_{-1}K_{+1} = oo$ and oe have antisymmetric rotational wavefunctions. Now, the nuclear wavefunction must be symmetric (ortho) to make Ψ_{total} antisymmetric. The $K_{-1} = 1, 3, 5, \dots$ ladders are ortho- H_2CO and have statistical weights that are 3 times higher than para- H_2CO levels.

H_2O is an example of a molecule with its dipole moment aligned with the principle axis of intermediate moment of inertia ($\mu_B \neq 0$). Therefore, the symmetric rotational wavefunctions have

$K_{-1}K_{+1} = ee$ and oo . The nuclear wavefunction must be antisymmetric (para) to make Ψ_{total} antisymmetric. Therefore, the energy levels, 0_{00} , 1_{11} , 2_{20} , etc. are para- H_2O . The antisymmetric rotational wavefunctions have $K_{-1}K_{+1} = eo$ and oe . The nuclear wavefunction must be symmetric (ortho) to make Ψ_{total} antisymmetric. Therefore, the energy levels, 1_{01} , 1_{10} , 2_{12} , 2_{21} , etc. are ortho- H_2O . Transitions between ortho- H_2O and para- H_2O levels are unlikely because the spin of H atoms would have to change.

4.2.2. Bose-Einstein Example - SO_2

Molecules containing two identical nuclei with even spin (e.g. N, O, etc.) have a total wavefunction that satisfy Bose-Einstein Statistics. Ψ_{total} must now be symmetric. In the case of SO_2 this eliminates certain energy levels! Sulfur Dioxide has its dipole moments along the intermediate principle axis ($\mu_B \neq 0$). Therefore, antisymmetric rotational wavefunctions have $K_{-1}K_{+1} = eo$ and oe . The spin of ^{16}O is 0. Therefore, the nuclear spin wavefunction can **only** be symmetric! Since Ψ_{total} must be symmetric, it is impossible to have antisymmetric rotational wavefunctions in the $^1\Sigma$ ground vibrational state of SO_2 . Only symmetric rotational wavefunctions exist with $K_{-1}K_{+1} = ee$ and oo (see Figure 14). For Bose-Einstein nuclei with spin > 0 , the nuclear wavefunction can be either symmetric and antisymmetric and all the rotational levels are permitted.

4.3. Hyperfine Structure - Asymmetric Top $^1\Sigma$ State

The hyperfine structure for asymmetric top molecules is analogous to symmetric top and linear molecules. Each $J_{K_{-1}K_{+1}}$ level is split. Calculation of the actual energy levels are much more complicated since the asymmetry of the molecule does not allow a single constant to describe the electric quadrupole and magnetic dipole coupling (you must use coupling tensors).

5. Linear Molecules with Electronic Angular Momentum

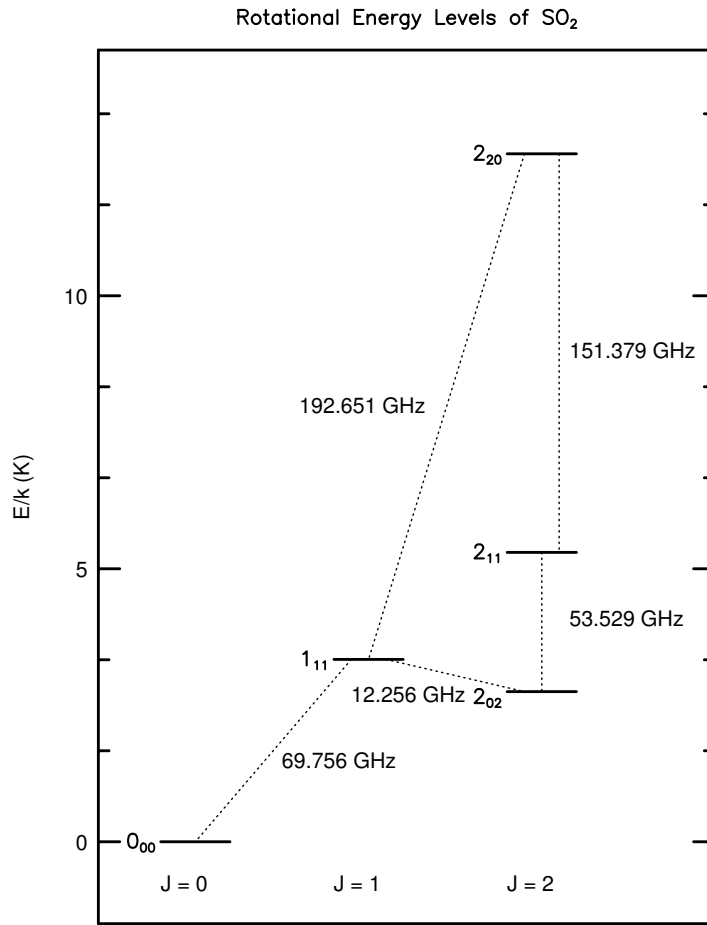


Fig. 19.— The rotational energy level diagram for SO₂. The vertical axis is energy above ground in K. All energy levels are displayed accurately. Since transitions between $K_{\pm 1}$ ladders are allowed, energy levels are organized by J. All energy levels up to $J = 2$ are shown. Notice that the 2_{02} level is lower in energy than 1_{11} .

REFERENCES

- Caselli, P., Myers, P. C., Thaddeus, P. 1995, *ApJ*, 455, L77
- Dore, L., Cazzoli, G., Caselli, P. 2001, *A&A*, accepted
- Edmonds, A.R. 1974, *Angular Momentum in Quantum Mechanics*, 3rd ed., (Princeton University Press: Princeton, New Jersey)
- Encrenaz, P.J., Wannier, P.G., Jefferts, K.B., Penzias A.A., & Wilson, R.W. 1973, *ApJL*, 186, 77
- Ferking, M.A., Langer, W.D. 1981, *J. Chem. Phys.*, 74, 6990
- Gerin, M., Pearson, J. C., Roueff, E., Falgarone, E., & Phillips, T. G. 2001, *ApJ*, 551, L193
- Gordy, W., Cook, R.L. 1984, *Microwave Molecular Spectroscopy* 3rd ed., in *Techniques of Chemistry* vol.17, (John Wiley & Sons:New York)
- Hollas, J. M. 1996, *Modern Spectroscopy*, 3rd ed., (John Wiley & Sons, New York)
- Ladd, E.F., Fuller, G.A., & Deane, J.R. 1998, *ApJ*, 496, 871
- Lovas, F.J. & Krupenie, P.H. 1974, *J. Phys. Chem. Ref. Data*, 3, 234
- Lovas, F.J. 1992, *J. Phys. Chem. Ref. Data*, 21, 181
- Kroto, H.W. 1992, *Molecular Rotation Spectra*, (Dover:Mineola, New York)
- Mauersberger, R., Wilson, T.L., Mezger, P.G., Gaume, R., & Johnston, K.J. 1992, *A&A*, 256,640
- Ramsey, N.F. 1953, *Nuclear Moments and Statistics*, in *Experimental Nuclear Physics* vol. I, ed. Segre, E., (John Wiley & Sons: New York)
- Rudolph, H.D. 1968, *Z. Naturforsch*, 23a, 540
- Townes, C.H., Schawlow, A.L., 1975, *Microwave Spectroscopy*, (Dover: New York)

Table 1. Parameters of Example Linear Molecules in $^1\Sigma$ States

Molecule	Name	B (GHz)	μ (D) ^a	Molecule	Name	B (GHz)	μ (D) ^a
CO	Carbon Monoxide	57.635968	0.11011	CS	Carbon Monosulfide	24.495562	1.957
¹³ CO		55.101011	0.11046	C ³⁴ S		24.103541	1.957
C ¹⁷ O		56.179990	0.11034	¹³ CS		23.123856	1.957
C ¹⁸ O		54.891420	0.11079	HCN	Hydrogen Cyanide	44.315975	2.984
HCO ⁺	Oxomethylum	44.5944	3.30	H ¹³ CN		43.170137	2.984
H ¹³ CO ⁺		43.37722	3.3	HC ¹⁵ N		43.02769	2.984
HC ¹⁸ O ⁺		42.58121	3.30	DCN		36.20746	2.984
DCO ⁺		36.01976	3.3	HNC	Hydrogen Isocyanide	45.33199	3.05
HOC ⁺	Hydroxymethylidynium	44.7349	4.0	HN ¹³ C		43.54561	2.699
N ₂ H ⁺	Diazenylium	46.586867	3.40	H ¹⁵ NC		43.02769	2.984
N ₂ D ⁺		38.554719	3.40	DNC		38.152998	3.050
SiO	Silicon Monoxide	21.711967	3.098	HC ₃ N	Cyanoacetylene	4.549058	3.724
HCS ⁺	Thioxomethylum	10.691406	1.86	HC ₅ N	Cyanodiacetylene	1.33133	4.37
HF	Hydrogen Flouride	616.365	1.826	HC ₇ N	Cyanoheptatriyne	0.5640007	5.0
C ₃ O	Tricarbon Monoxide	4.8108809	2.391	HC ₉ N	Cyanoocatetrayne	0.2905183	5.6
OCS	Carbonyl Sulfide	6.0814921	0.715	HC ₁₁ N	Cyanodecapentayne	0.1690629	6.2

^aD = Debye. 1D = 10⁻¹⁸esu (cgs units).

References. — All data from JPL line catalog

Table 2. Properties of Astrophysically Important Nuclei and Hyperfine Coupling Constants of Astrophysically Important Molecules

Isotope	Spin I	Magnetic Moment ^a	Quadrupole Moment ^b	Molecule	eQq (MHz)	C _I (kHz)	Ref
¹ H	$\frac{1}{2}$	+2.79278	...				
² D	1	+0.85743	+0.0028	DCN	+0.1944	−0.6	1
¹² C	0				
¹³ C	$\frac{1}{2}$	+0.7024	...				
¹⁴ N	1	+0.4036	+0.01				
				NH ₃	−4.0842		1
				HCN	−4.7091	+10.4	1
				HC ₃ N	−4.28		1
				CH ₃ CN	−4.2244		1
¹⁵ N	$\frac{1}{2}$	−0.2831	...				
¹⁶ O	0				
¹⁷ O	$\frac{5}{2}$	−1.8937	−0.026				
				C ¹⁷ O	+4.337	−30.4	2
				HC ¹⁷ O ⁺	+4.595	−20	3
¹⁸ O	0				
²⁸ Si	0				
³² S	0				
³³ S	$\frac{3}{2}$	+0.6434	−0.055				
				C ³³ S	+12.83		1
³⁴ S	(0)				

^aMagnetic Moment in nuclear magnetons. $1\mu_B = 9.274 \times 10^{-21}$ erg·gauss^{−1}.

^bQuadrupole Moment in barns. 1 barn = 10^{-24} cm².

References. — 1. Gordy & Cook 1984; 2. Frerking & Langer 1981; 3. Dore et al. 2001;

Table 3. Frequencies for Hyperfine Components of HCN and C¹⁷O

Molecule	J_i	J_f	F_i	F_f	$\Delta\nu_Q^a$ (kHz)	$\Delta\nu_M^a$ (kHz)	Δv (km s ⁻¹)	ν (GHz)	Relative Intensity	
HCN	1	0						88.631602		
			2	1	+235.4	+10.4	-0.83	88.631848	0.555	
			1	1	-1177.3	-10.4	+4.02	88.630414	0.333	
			0	1	+2354.5	-20.8	-7.90	88.633936	0.111	
	2	1							177.261111	
			3	2	+100.9	+10.4	-0.19	177.261222	0.467	
			2	2	-1412.7	-20.8	+2.43	177.259677	0.083	
			2	1	0	0	0	177.261111	0.250	
			1	2	+941.82	-41.6	-1.52	177.262011	0.005	
			1	1	+2354.5	-20.8	-3.95	177.263445	0.083	
1			0	-1177.3	-10.4	+2.01	177.259923	0.111		
C ¹⁷ O	1	0						112.359275		
			7/2	5/2	-216.8	-76.0	+0.78	112.358982	0.444	
			5/2	5/2	+693.9	+30.4	-1.93	112.359999	0.333	
			3/2	5/2	-607.2	+106.4	+1.34	112.358774	0.222	
	2	1							224.714368	
			9/2	7/2	-92.9	-76.0	+0.22	224.714199	0.333	
			7/2	7/2	+743.5	+60.8	-1.07	224.715172	0.095	
			7/2	5/2	-167.3	-45.6	+0.28	224.714155	0.171	
			5/2	7/2	+526.6	+167.2	-0.93	224.715062	0.016	
			5/2	5/2	-384.1	+60.8	+0.43	224.714045	0.122	
			5/2	3/2	+917.0	-15.2	-1.20	224.715270	0.062	
3/2	5/2	-1003.7	+136.8	+1.16	224.713501	0.040				
3/2	3/2	+297.4	+60.8	-0.48	224.714726	0.093				
1/2	3/2	-260.2	106.4	+0.20	224.714214	0.067				

^aQuadrupole ($\frac{E_Q}{h}$) and magnetic ($\frac{E_M}{h}$) hyperfine frequency shifts with respect to the Lovas unshifted frequency

Table 4. Parameters of Example Symmetric Top Molecules

Molecule	Name	A (GHz)	B (GHz)	C (GHz)	μ_A (D)	μ_B (D)	μ_C (D)
NH ₃	Ammonia	B	298.11706	186.72636	0	0	1.476
CH ₃ CCH	Methyl Acetylene	158.590	8.54586	B	0.75	0	0
CH ₃ CN	Methyl Cyanide	158.0990	9.1989	B	3.92197	0	0
H ₃ O ⁺	Hydronium Ion	337.38849	B	181.3740	0	0	1.44

Table 5. Parameters of Example Asymmetric Top Molecules

Molecule	Name	A (GHz)	B (GHz)	C (GHz)	κ	μ_A (D)	μ_B (D)	μ_C (D)
H ₂ CO	Formaldehyde	281.97058	38.833987	34.004244	-0.96	2.331	0	0
H ₂ CS	Thioformaldehyde	291.291641	17.699628	16.651830	-0.99	1.649	0	0
CH ₃ OH	Methanol	127.484	24.67998	23.76970	-0.98	0.885	1.440	0
HNCO	Isocyanic Acid	912.711435	11.0710098	10.9105763	~ -1	1.6020	1.3500	0
H ₂ O	Water	835.8403	435.3517	278.1387	-0.44	0	1.84718	0
HDO		701.9315	272.9126	192.0552	-0.68	0.657	1.732	0
SO ₂	Sulfer Dioxide	60.778550	10.318074	8.799703	-0.94	0	1.6331	0
t-HCOOH	trans-Formic Acid	77.51225	12.05511	10.41612	-0.95	1.396	0.260	0
CH ₃ OCH ₃	Dimethyl Ether	38.7882	10.0565	8.8868	-0.92	0	1.302	0
NH ₂ D	Dueterated Ammonia	290.125	192.194	140.795	-0.31	-0.18	0	1.463

Table 6. Selection Rules for Asymmetric Top Molecules

Electric Dipole	Inertia Component	Allowed Transitions $(K_{-1}K_{+1})_i \leftrightarrow (K_{-1}K_{+1})_f$	ΔK_{-1}	ΔK_{+1}
$\mu_A \neq 0$	least	$ee \leftrightarrow eo^a$ $oe \leftrightarrow oo$	$0, \pm 2, \dots$	$\pm 1, \pm 3, \dots$
$\mu_B \neq 0$	intermediate	$ee \leftrightarrow oo$ $oe \leftrightarrow eo$	$\pm 1, \pm 3, \dots$	$\pm 1, \pm 3, \dots$
$\mu_C \neq 0$	greatest	$ee \leftrightarrow oe$ $eo \leftrightarrow oo$	$\pm 1, \pm 3, \dots$	$0, \pm 2, \dots$

^ae = even and o = odd

Table 7. Behavior of Rotational Wavefunction with π rotation about the Principle Axes

$K_{-1}K_{+1}$ ^a	$J_{K_{-1}K_{+1}}$ Symmetry ^b		
	A	B	C
ee	+	+	+
eo	+	–	–
oo	–	+	–
oe	–	–	+

^ae = even and o = odd

^b+ = symmetric and – = antisymmetric for rotational of π about the principle axes A, B, or C.

Table 8. Summary of Quantum Numbers

Electronic State	Molecule	Special Cases	Hyperfine ^a	Quantum Numbers	Astrophysical Example	
¹ Σ	Linear		S	J	CO	
			M	J F	C ¹⁷ O	
	Symmetric Top	Inversion		M	J F ₁ (... F _n) F	N ₂ H ⁺
				S	J _K	
		<i>C</i> _{3v} Symmetry		S	J _K F	NH ₃
				S	J _K [±] or inv(J,K)	CH ₃ CCH
	Asymmetric Top	Torsion		S	J _K A and J _K E	CH ₃ CN
				S	J _K A F and J _K E F	CH ₃ OH
		Inversion		S	J _K A [±] and J _K E	H ₂ CO
				S	J _{K-1K+1}	HNCO
			S	J _{K-1K+1} F	NH ₂ D	
			S	J [±] _{K-1K+1} F		
² Σ	Linear		S	N _J	CO ⁺	
			S	N _J F	CN	
	Asymmetric Top		S	N _{KK} F	CH ₂ ⁺	
³ Σ	Linear		S	N _J	SO	
			S	N _J F		
² Π	Linear ^c			J _(Ω) [±]		
				J _(Ω) [±] F	OH	

^aS = single coupling nucleus. M = multiple coupling nuclei.

^b() = optional.

^cSince electronic transitions are not common in molecular clouds, the Ω subscript is usually dropped. Furthermore, each Π state is split into different Ω states. For the case of above, there are energy levels for ²Π_{3/2} and ²Π_{1/2}.